Journal of
Medicinal Chemistry

Article

Metabolic activation of pirfenidone mediated by cytochrome P450s and sulfotransferases

Shenzhi Zhou, Wei Li, Min Tian, Na Zhang, Xiaojing Yang, Weiwei Li, Ying Peng, and Jiang Zheng

J. Med. Chem., **Just Accepted Manuscript** • DOI: 10.1021/acs.jmedchem.9b02073 • Publication Date (Web): 09 Jul 2020

Just Accepted

is published by the American Chemical Society. 1155 Sixteenth Street N.W., Washington, DC 20036

Metabolic activation of pirfenidone mediated by cytochrome P450s and sulfotransferases

Shenzhi Zhou,[†] Wei Li,[†] Min Tian,[†] Na Zhang,[†] Xiaojing Yang,[†] Weiwei Li,*[‡] Ying Peng,*[†] and Jiang Zheng*[†‡§]

[†]Wuya College of Innovation, Shenyang Pharmaceutical University, Shenyang, Liaoning 110016, P. R. China

[‡]State Key Laboratory of Functions and Applications of Medicinal Plants, Guizhou Provincial Key Laboratory of Pharmaceutics, Guizhou Medical University, Guiyang, Guizhou 550025, P. R. China

[§]Key Laboratory of Environmental Pollution, Monitoring and Disease Control (J.Z.), Ministry of Education, Guizhou Medical University, Guiyang, 550025, P. R. China

Corresponding Authors

Jiang Zheng, PhD

Wuya College of Innovation, Shenyang Pharmaceutical University, No. 103, Wenhua Road, Shenyang, Liaoning, 110016, P. R. China

State Key Laboratory of Functions and Applications of Medicinal Plants, Key Laboratory of Pharmaceutics of Guizhou Province, Guizhou Medical University, 9 Beijing Road, Guiyang, Guizhou, 550004, P. R. China

Email: zhengneu@yahoo.com

Tel: +86-24-23986361; Fax: +86-24-23986510

Ying Peng, PhD

Wuya College of Innovation, Shenyang Pharmaceutical University, No. 103, Wenhua Road, Shenyang, Liaoning, 110016, P. R. China

Email: yingpeng1999@163.com

Tel: +86-24-23986361; Fax: +86-24-23986510

Weiwei Li, PhD

Guizhou Provincial Key Laboratory of Pharmaceutics, Guizhou Medical University, 9 Beijing Road, Guiyang, Guizhou, 550004, P. R. China

Email: weiweili0615@163.com

Tel: +86-24-23986361; Fax: +86-24-23986510

ABSTRACT

Pirfenidone is approved for the treatment of idiopathic pulmonary fibrosis. Idiosyncratic drug reactions, due to clinical application of pirfenidone, have been documented, even along with death cases resulting from acute liver failure. The present study aimed at the investigation of metabolic activation of pirfenidone possibly participating in the reported adverse reactions. Pirfenidone-derived GSH/NAC conjugates were detected in microsomal/primary hepatocyte incubations after exposure to pirfenidone. The GSH/NAC conjugates were also observed in bile and urine of rats given pirfenidone, respectively. The observation of the conjugates suggests the formation of a quinone methide intermediate derived from pirfenidone. The intermediate was possibly generated through two pathways. First, pirfenidone was directly metabolized to the quinone methide intermediate via dehydrogenation; second, pirfenidone was oxidized to 5-hydroxymethyl pirfenidone, followed by sulfation to a benzyl alcohol-sulfate derivative. The findings facilitate the understanding of the mechanisms of pirfenidone-induced idiosyncratic toxicity and assist medicinal chemists to minimize toxicities in the development of new pharmaceutical agents.

INTRODUCTION

Idiopathic pulmonary fibrosis (IPF) is a severe form of fibrosing interstitial pneumonia, which may cause progressive loss of pulmonary functions and eventually respiratory failure.[1] The pathogenic factors of IPF are perplexing, including but not limited to cigarette smoking, breathing dust, viral infections and exposures to the contaminated environment.[2] Briefly, the micro-injuries mentioned above disturb lung repeatedly, resulting in death of epithelial cells. Then an inordinate wound healing leads to imbalance between fibrotic and anti-fibrotic factors, which is involved in excessive proliferation of myofibroblasts, and then the progressive remodeling results in IPF ultimately.[1,3]

Pirfenidone (5-methyl-1-phenyl-1*H*-pyridine-2-one, **1**), a pyridone derivative, has been authorized for the treatment of IPF in Japan, Europe, the United States, China, and other countries.[4] Pirfenidone is considered to exert an anti-fibrotic effect via the reduction of transforming growth factor-β1, a pro-inflammatory and profibrotic cytokine. Inhibition of other pro-inflammatory cytokines such as tumor necrosis factor-α also contributes to its anti-inflammatory property.[5,6] As an anti-oxidant, pirfenidone can scavenge hydroxyl radical and superoxide anion.[7,8] The recommended oral dosage of pirfenidone is 801 mg a day in the first week, then the dose is elevated to 1,602 mg/day in the second week, and final therapy is invariable to 2,403 mg/day (801 mg taken 3 times) from 15th day onwards.[9,10] The most common side effects of pirfenidone include gastrointestinal reactions, photosensitization, and elevation of serum ALT/AST and bilirubin.[9-11] It was reported that 2.9% of patients

showed increased serum ALT/AST activities 3-fold greater than that of normal upper limits.[11] In 2017, a 77-year-old patient taking pirfenidone 600 mg/day was reported to die, due to suffering acute liver failure.[12] Another death case resulting from pirfenidone-related acute liver failure was documented in 2019.[13]

Previous studies indicated that pirfenidone is mainly metabolized by cytochrome P450 enzymes, especially CYP1A2.[9] Pirfenidone can be oxidized to 5-hydroxymethyl pirfenidone (5-hydroxymethyl-1-phenyl-1*H*-pyridine-2-one, **2**) by hydroxylation of the methyl group, followed by further oxidation to a more polar metabolite, 5-carboxy pirfenidone.[9] Pirfenidone and 5-carboxy pirfenidone can also undergo glucuronidation.[9,14]

Sulfation, catalyzed by sulfotransferases (SULTs), is one of phase II conjugation pathways responsible for metabolism of various endogenous and exogenous molecules.[15,16] SULTs catalyze the transfer of a sulfonyl group from 3′-phosphoadenosine-5′-phosphosulfate (PAPS) to an amino, hydroxyl or sulfhydryl group of substrates.[17] Like many drug metabolizing enzymes, SULTs tend to increase hydrophilicity of substances and thus facilitate their excretion in urine. However, SULTs are reportedly involved in bioactivating certain compounds *in vivo*, especially for allylic alcohols, benzyl alcohols, and aromatic hydroxylamines.[15,17] Sulfate is a good leaving group, and the departure of the sulfonyl group may produce reactive electrophilic intermediates, which may result in potential toxicities.[18,19] For example, aloe-emodin was reported to be metabolized to the corresponding sulfate by SULTs,

which possibly induces cytotoxicity to HepG2 cells.[20] SULT-mediated metabolism of lucidin was found to generate an electrophilic metabolite that reacts with DNA.[21]

Idiosyncratic drug reactions (IDRs) vary from individual to individual, and it is difficult to reproduce IDRs in preclinical research for the lack of generally applicable animal models. IDRs are almost the most unpredictable risk in the drug development phase.[22] Because of their puzzling uniqueness and low occurrence, IDRs are usually not observed until drugs are extensively consumed in patient population, which means both a great loss of resources for the pharmaceutical industry and a fatal threat for patients.[22-24] Although most side effects of pirfenidone are tolerable and reversible by drug discontinuation, the common anaphylactic reactions, such as photosensitization, drug eruption, and drug induced lupus erythematosus, particularly along with 2 death cases resulting from pirfenidone-related acute liver failure, have been catching our attention. The recommended daily doses[9,10] of pirfenidone are quite high, not only for the maximum (2,403 mg/day) but also for the minimum (801 mg/day), which increases the risk of idiosyncratic toxicity.[25,26] Although the incidence of idiosyncratic effect of pirfenidone is rare, its consequence is fatal and the mechanisms of its toxic action remain unknown. Idiosyncratic toxicity is considered to be associated with metabolic activation and immune-mediation.[22,27-29] Thus we initiated the investigation to determine whether pirfenidone is bioactivated and to define the metabolic pathways involved in the metabolic activation of pirfenidone.

RESULTS

Metabolic activation of pirfenidone by P450 enzymes.

As an initial step, we incubated **1** in rat liver microsomes (RLMs) fortified with cofactor NADPH and trapping agent glutathione (GSH) or *N*-acetylcysteine (NAC). At least triplet experiments were conducted in all *in vitro* studies to exclude contingency. A chromatographic peak with a retention time at 7.25 min was observed by monitoring precursor/product (Q1/Q3) ion pair *m*/*z* 202/77 tentatively responsible for compound **2**, a primary oxidative metabolite of pirfenidone (Figure 1).

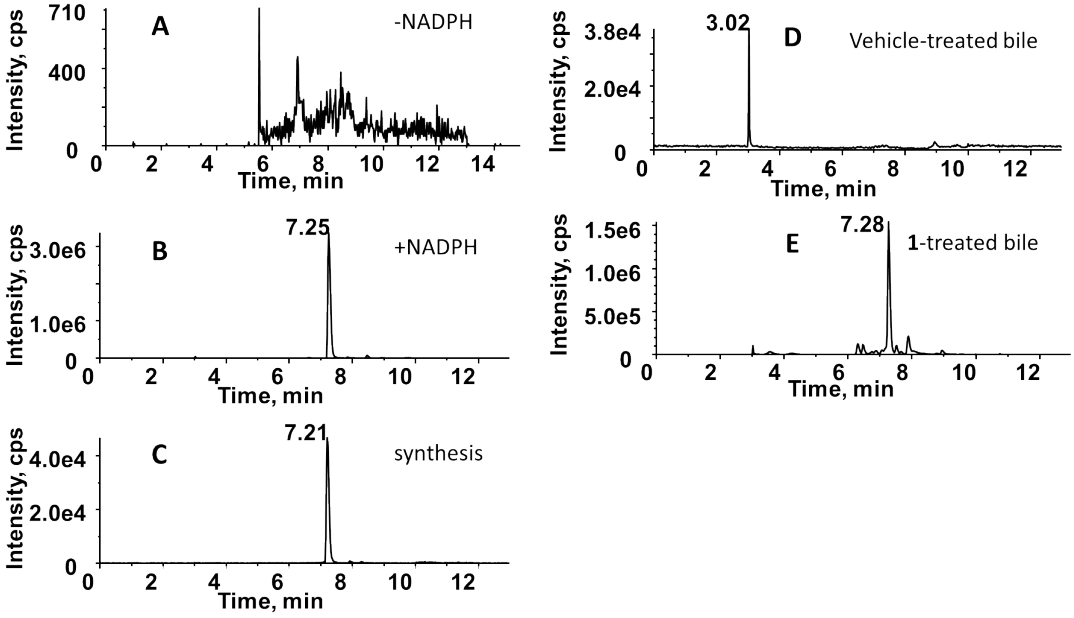

Figure 1. Characterization of metabolite **2**. Extracted ion (*m*/*z* 202/77) chromatograms obtained from LC-MS/MS analysis of RLM incubations of **1** in the absence (A) or presence (B) of NADPH. Extracted ion (*m*/*z* 202/77) chromatogram obtained from analysis of bile collected from vehicle-treated (D) or **1**-treated (E) rats and of synthetic **2** (C).

To verify the structure of the oxidative metabolite, compound **2** was chemically synthesized by hydration of 5-bromomethyl-1-phenyl-1*H*-pyridine-2-one (P-Br, refer to Experimental Section **2.1.**, Scheme 4). Compound **2** was successfully synthesized

and characterized by mass spectrometry and NMR (refer to Experimental Section **2.1.**). As expected, synthetic **2** shared similar retention time and fragmentation pattern with the one observed in microsomal incubations. This allowed us to ensure the metabolic hydroxylation of the methyl group on pyridone ring of **1** to **2**.

A pirfenidone-derived GSH conjugate (**10**, Scheme 1) with a retention time at 6.6 min (Figure 2) was detected in GSH-fortified RLM incubations by acquiring Q1/Q3 ion pair *m*/*z* 491/184 in positive mode (Figure 2B). The tandem mass spectrometric (MS/MS) spectrum of GSH conjugate **10** was obtained by acquiring enhanced product ion (EPI) scanning with a range of *m*/*z* 50 to 550 (Figure 2D). The mass spectrum of the GSH conjugate was quite simple with limited fragments. The most abundant fragment generated was ion *m*/*z* 184 resulting from the cleavage of the S−C bond from the GSH moiety. And fragment ion at *m*/*z* 218 came from the cleavage of the C−S bond of the GSH moiety. The neutral loss of the *γ*-glutamyl moiety from *m*/*z* 491 led to the production of fragment ion *m*/*z* 362. The characteristic fragment ion at *m*/*z* 156 resulted from the elimination of CO from the pirfenidone portion.

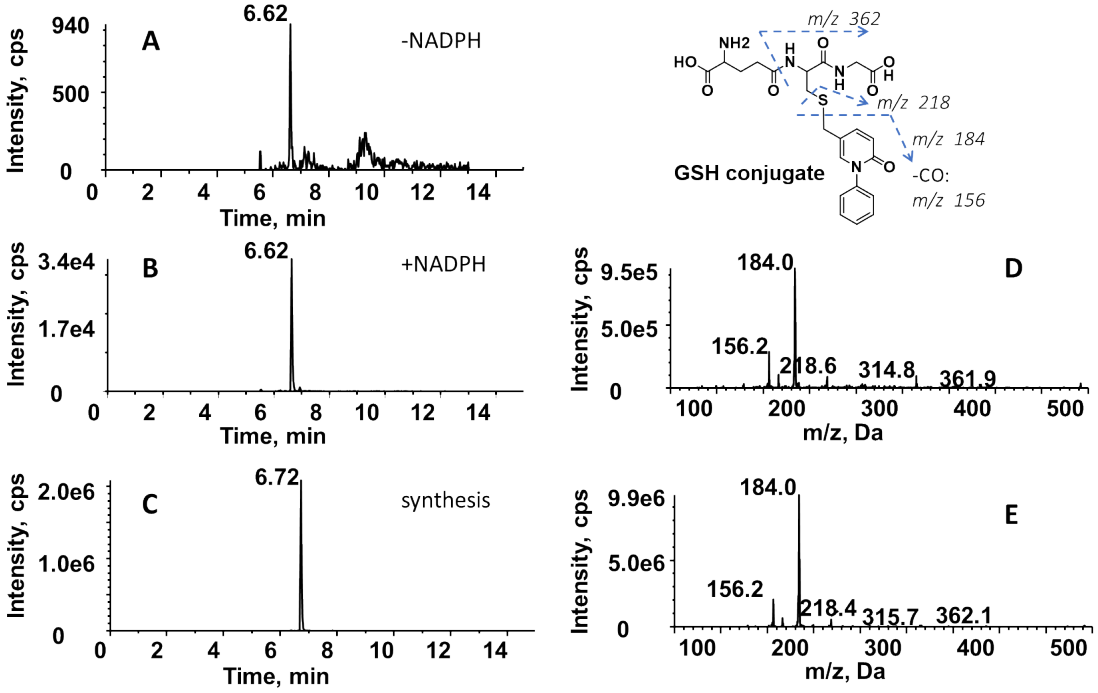

Figure 2. Characterization of GSH conjugate **10** generated in microsomal incubations. Extracted ion (*m*/*z* 491/184) chromatograms obtained from LC-MS/MS analysis of RLM incubations of **1** fortified with GSH in the absence (A) or presence (B) of NADPH. D: MS/MS spectrum of GSH conjugate **10** produced in RLM incubations. Extracted ion (*m*/*z* 491/184) chromatogram (C) and MS/MS spectrum (E) of synthetic GSH conjugate **10**.

Pirfenidone-derived NAC conjugate **11** (Scheme 1) was detected at the retention time of 7.26 min by acquiring Q1/Q3 ion pair *m*/*z* 347/184 (Figure 3B). EPI scanning was employed to acquire the MS/MS spectrum of NAC conjugate **11** as well (Figure 3D). Again, ion *m*/*z* 184 was found to be the most abundant fragment for the NAC conjugate, which was from the cleavage of S−C bond of **1**. NAC conjugate **11** showed similar fragmentation pattern as GSH conjugate **10**, such as fragment ions *m*/*z* 218 and 156 derived from the cleavage of C−S bond attached with the NAC moiety and from the pirfenidone moiety, respectively. No such GSH and NAC conjugates were observed in NADPH-free incubations. This suggests that the formation of the two

metabolites was NADPH-dependent, implicating the involvement of P450s in the generation of the pirfenidone-derived reactive metabolites.

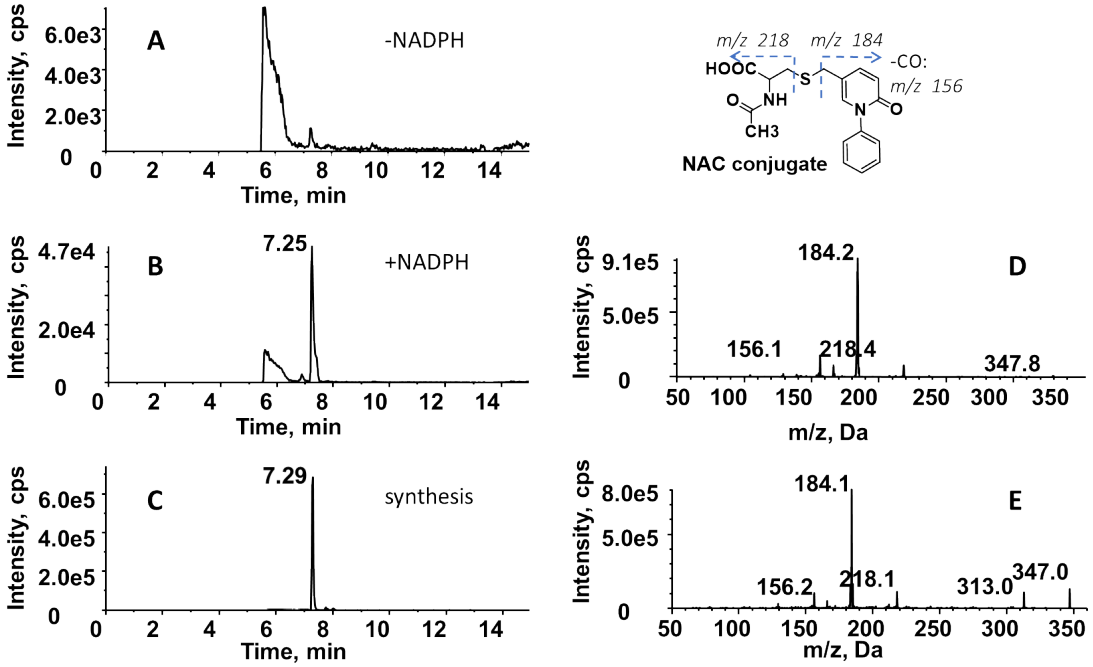

Figure 3. Characterization of NAC conjugate **11** generated in microsomal incubations. Extracted ion (*m/z* 347/184) chromatograms obtained from LC-MS/MS analysis of RLM incubations of **1** fortified with NAC in the absence (A) or presence (B) of NADPH. D: MS/MS spectrum of NAC conjugate **11** produced in RLM incubations. Extracted ion (*m/z* 347/184) chromatogram (C) and MS/MS spectrum (E) of synthetic NAC conjugate **11**.

Chemical synthesis was executed to verify the structure of the GSH and NAC conjugates above. The synthetic products were analyzed by LC-MS/MS and Q-TOF MS. The retention times and MS/MS spectra of the synthetic conjugates were similar as those of the GSH/NAC conjugates detected the *in vitro* and *in vivo* studies (Figures 2C/2E, 3C/3E, 6C/6E, 7C/7E, 8C/8E). The structure of GSH conjugate **10** was further confirmed by NMR (refer to Experimental Section **2.2.**).

Scheme 1. Proposed pathways of metabolic activation of pirfenidone.

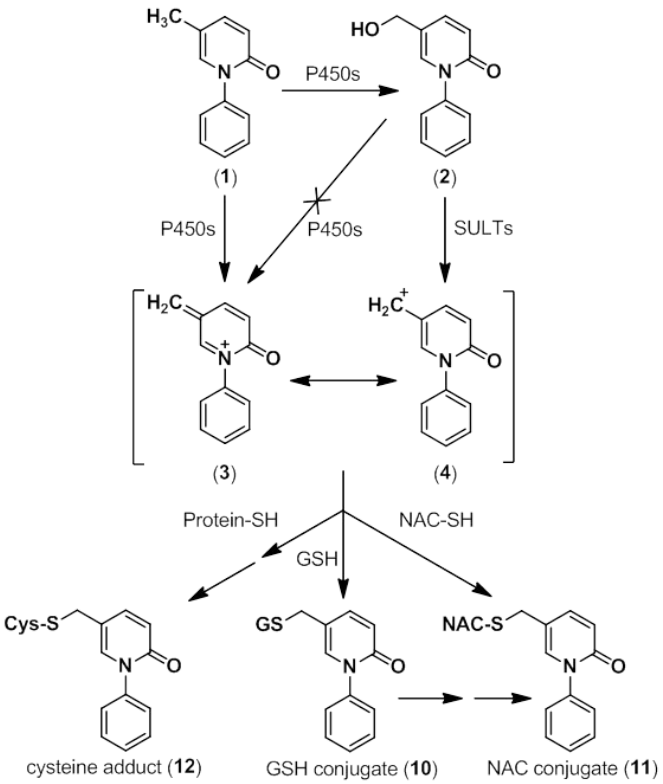

P450 enzymes responsible for metabolic activation of 1.

Human recombinant P450s 1A2, 2A6, 2B6, 2C9, 2C19, 2D6, 2E1, 3A4, and 3A5 were individually incubated with **1** supplemented with NADPH and GSH. The catalytic capabilities of these enzymes were evaluated by monitoring the formation of GSH conjugate **10**. The results shown in Figure 4A demonstrated that CYP3A4 dominated the catalysis responsible for the formation of quinone methide **3** (by monitoring GSH conjugate **10**), closely followed by CYP3A5. Figure 4B describes the graphic contribution of each P450 enzymes to the metabolic activation after normalization, according to their natural abundance in human liver microsomes.[31] CYP3A4 contributed the most to the formation of quinone methide **3**, followed by CYP2A6 and CYP1A2.

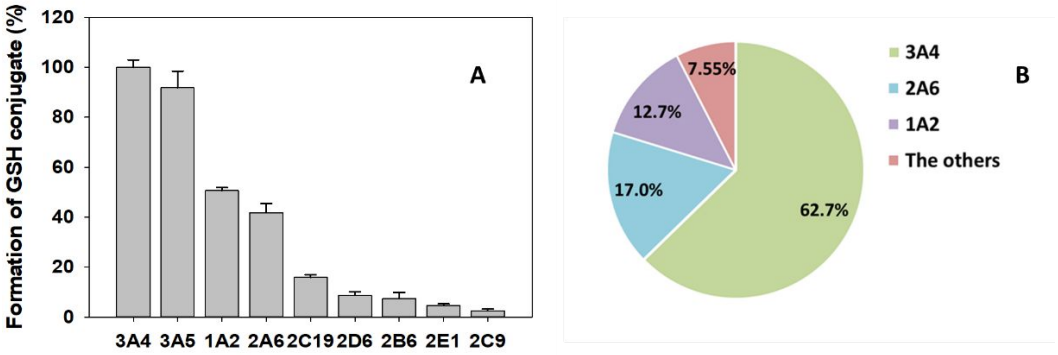

Figure 4. Role of individual human recombinant P450 enzymes in metabolic activation of pirfenidone. A: Formation of GSH conjugate **10** in incubations of **1** with nine individual human recombinant P450 enzymes was measured by LC-MS/MS. The most abundant GSH conjugate **10** detected was normalized to 100%; B: The contribution of each P450 enzyme was calculated based on the formation of GSH conjugate **10** after normalization, according to the natural abundance of the corresponding P450 enzymes in human liver microsomes. Data represent the mean ± SD (n = 3).

Metabolic activation of 1 and 2 in primary hepatocytes.

Bioactivation studies were also conducted in cultured rat primary hepatocytes. Freshly isolated hepatocytes were incubated with parent drug **1** or primary metabolite **2**. As expected, GSH conjugate **10** was detected in the cell culture system after exposure to **1** (Figure 5B). Interestingly, GSH conjugate **10** was also found in **2**-treated hepatocytes (Figure 5C).

In a separate study, cells were respectively preincubated with ketoconazole (KTC, a selective CYP3A inhibitor), 2,6-dichloro-4-nitrophenol (DCNP, an inhibitor of SULTs), or vehicle (0.1 % DMSO), followed by treatment with **1** and assessment of GSH conjugate **10** by LC-MS/MS. GSH conjugate **10** detected in vehicle-pretreated group was normalized as 100%. As depicted in Figure 6B, KTC pretreatment resulted in 74% inhibition of the formation of GSH conjugate **10**, and DCNP caused 32% inhibition of the generation of the GSH conjugate. Similar inhibition study was

performed to define the metabolic pathways of **2**. The presence of DCNP was found to attenuate the formation of GSH conjugate **10** by 51% in **2**-treated hepatocytes (Figure 6A).

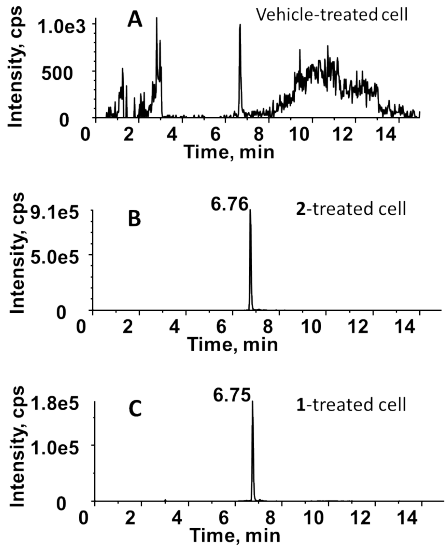

Figure 5. Characterization of GSH conjugate **10** generated in primary hepatocytes. Extracted ion (*m*/*z* 491/184) chromatograms obtained from LC-MS/MS analysis of rat primary hepatocytes treated with vehicle (A), **2** (B) or **1** (C).

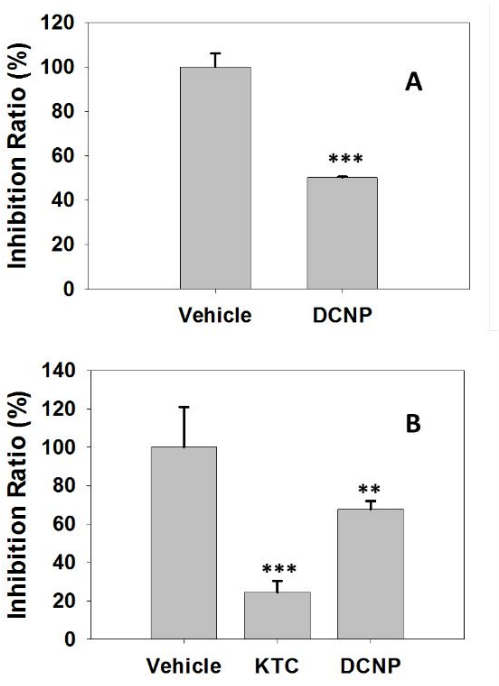

Figure 6. Inhibitory effects of KTC and DCNP on the generation of GSH conjugate **10** in primary hepatocytes. The formation of GSH conjugate **10** in primary hepatocytes

pretreated with vehicle was normalized to 100%. A: Formation of GSH conjugate **10** in **2**-treated primary hepatocytes which were pretreated with vehicle or DCNP; B: Formation of GSH conjugate **10** in **1**-treated primary hepatocytes which were respectively pretreated with vehicle, KTC, or DCNP. Data represent the mean ± SD (n=3). ***$p < 0.005$ (mean ± SD).

Formation of reactive metabolite of 1 via sulfation.

To further verify the speculated sulfation route participating in the bioactivation of **2**, we incubated synthetic **2** with rat liver cytosol (RLC) fortified with GSH or NAC in the presence of SULT cofactor PAPS. As expected, the corresponding GSH and NAC conjugates were both detected in PAPS-spiked RLC incubations (Figure 7E and Figure S1E). No such conjugates were observed in vehicle-spiked incubations. The observed PAPS-dependent formation of the GSH/NAC conjugates from **2** provided strong evidence for the participation of sulfation in the metabolic activation of **2**.

An *in vitro* two-step incubation was carried out to further define the metabolic pathway of pirfenidone bioactivation. Compound **1** was incubated with RLMs supplemented with NADPH, and the resultant incubation mixture which contains **2** (confirmed by the above experiment) was mixed with the secondary incubation mixture containing RLC and GSH, followed by incubation at 37 °C. GSH conjugate **10** was detected in the resulting incubation mixture (Figure 7). Noteworthy, the incubation spiked with PAPS offered approximately 2.5-fold increase in the formation of GSH conjugate **10**, relative to that of the incubation spiked with vehicle (Figures 7B and 7C).

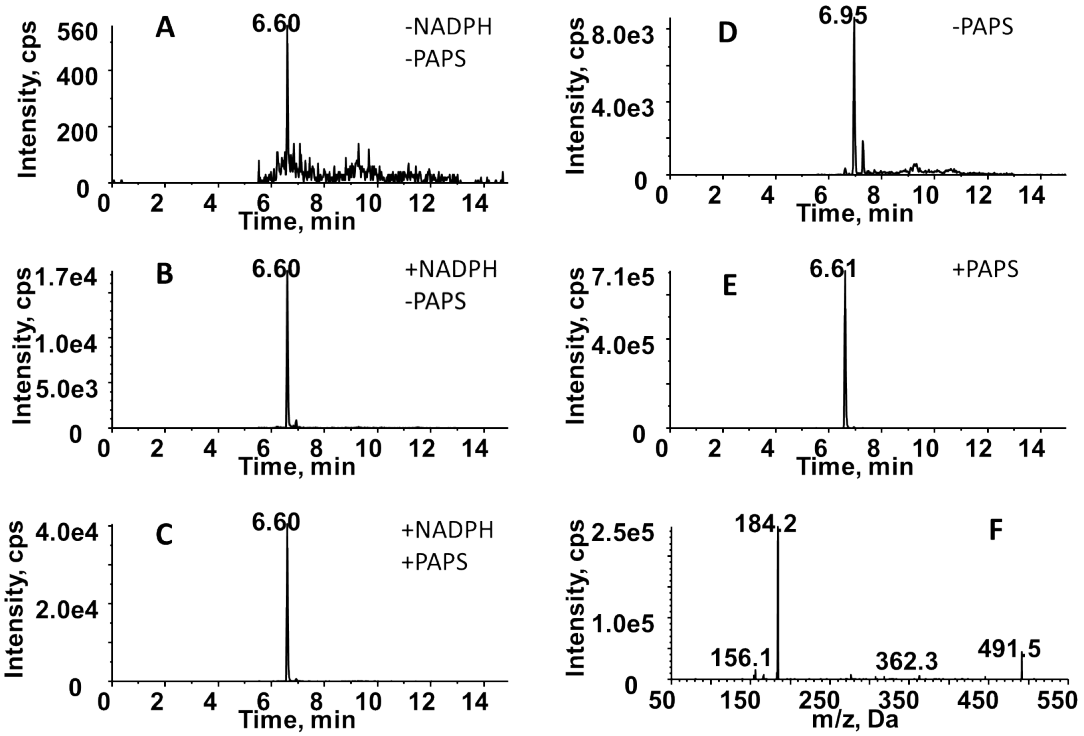

Figure 7. Characterization of GSH conjugate **10** generated in RLC and RLM-RLC incubation systems. Extracted ion (*m*/*z* 491/184) chromatograms obtained from LC-MS/MS analysis of GSH-fortified RLM-RLC incubations of **1** without NADPH or PAPS (A), with NADPH but without PAPS (B), and with NADPH and PAPS (C). Extracted ion (*m*/*z* 491/184) chromatograms obtained from LC-MS/MS analysis of RLC incubations containing **2** and GSH in the absence (D) or presence (E) of PAPS. F: MS/MS spectrum of GSH conjugate **10** produced in **2**-fortified RLC incubation.

Biliary and urinary metabolites derived from 1

In order to determine the metabolic activation of pirfenidone *in vivo*, biliary and urinary GSH-related metabolites were determined by LC-MS/MS. GSH and NAC conjugates **10** and **11** were detected in bile of rats treated with **1** (Figures 8B/8D, S2B). Abundant urinary NAC conjugate **11** was observed in rats given **1** (Figures 9B/9D). The two conjugates showed consistent mass spectral fragment patterns and retention times with the synthetic conjugates as well as those of the corresponding metabolites

detected in *in vitro* incubations. No such conjugates were observed in vehicle-treated animals.

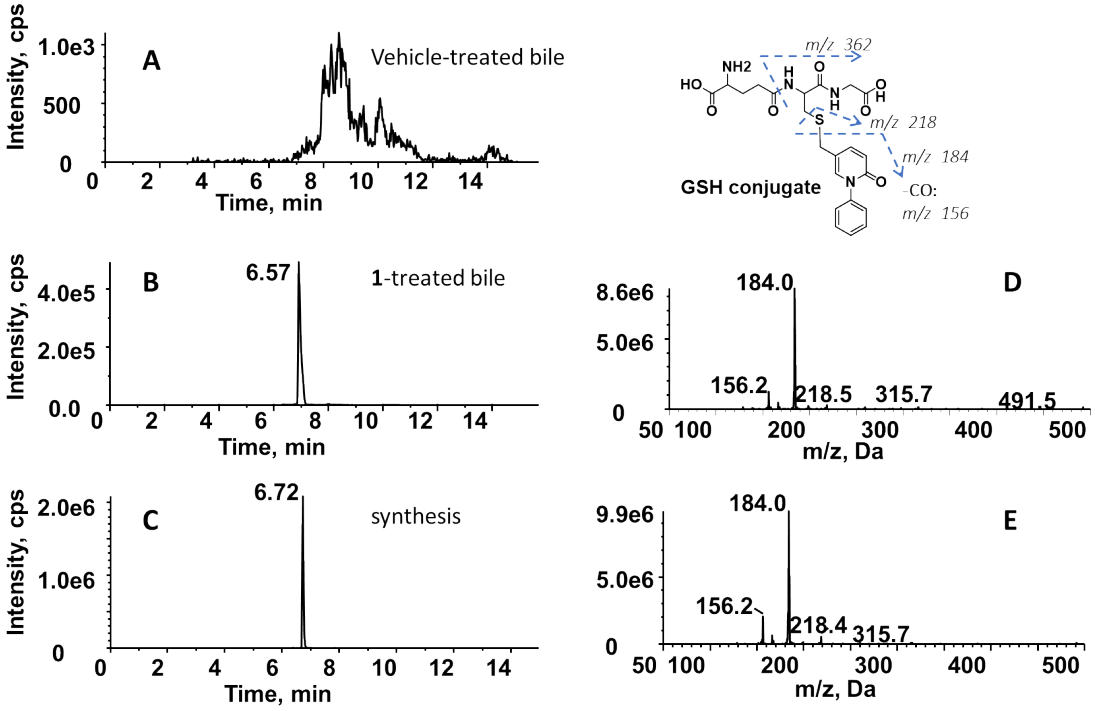

Figure 8. Characterization of biliary GSH conjugate **10**. Extracted ion (*m*/*z* 491/184) chromatograms obtained from LC-MS/MS analysis of bile collected from vehicle-treated (A) and **1**-treated (B) rats. D: MS/MS spectrum of GSH conjugate **10** obtained from bile of rats treated with **1**. Extracted ion (*m*/*z* 491/184) chromatogram (C) and MS/MS spectrum (E) of synthetic GSH conjugate **10**.

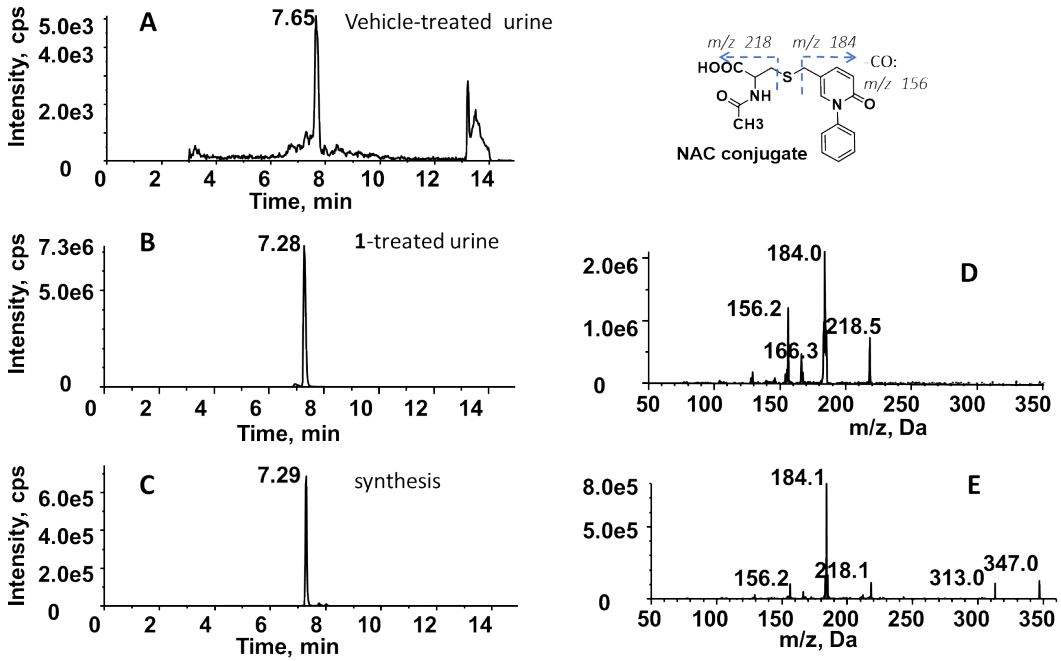

Figure 9. Characterization of urinary NAC conjugate **11**. Chromatograms of extracted ion (*m*/*z* 347/184) obtained from LC-MS/MS analysis of urine of vehicle-treated (A) and **1**-treated (B) rats. D: MS/MS spectrum of NAC conjugate **11** detected in urine of rats treated with **1**. Extracted ion (*m*/*z* 347/184) chromatogram (C) and MS/MS spectrum (E) of synthetic NAC conjugate **11**.

Saturation of hepatic GSH conjugate 10 formation

We measured hepatic GSH conjugate **10** in mice treated with pirfenidone at various dosages. As depicted in Figure 10, the formation of hepatic GSH conjugate **10** significantly increased with the increase of doses administered in mice at doses from 10 to 100 mg/kg. After that, the levels of GSH conjugate **10** reached a plateau with the elevation of doses, i.e. 200, 300, and 400 mg/kg. Clearly, there is certain capacity for the formation of the reactive metabolites resulting from pirfenidone metabolism as well as for the generation of GSH conjugation.

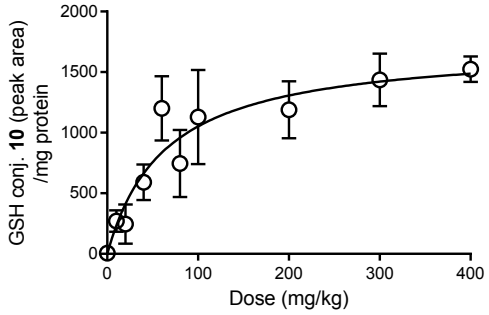

Figure 10. Dose-dependent formation of hepatic GSH conjugate **10**. Levels of GSH conjugate **10** was measured in liver samples harvested from mice given **1** at various doses after 0.5 h treatment. Data represent the mean ± SD (n=3).

Protein covalent modification by reactive metabolites of 1

Electrophilic metabolites may cause protein covalent binding, which is regarded to trigger the progression of cytotoxicity. To determine the protein modification, we decided to completely digest protein samples and analyze the resulting cysteine adduct. We succeeded in the detection of a cysteine adduct in proteolytic protein samples obtained from liver tissues of mice treated with **1**. The cysteine adduct eluted at retention time of 6.24 min, and the Q1/Q3 ion pair monitored was *m*/*z* 305/184 (Figures 10B/10D). The MS/MS spectrum demonstrated base fragment ion at *m*/*z* 184, possibly resulting from the elimination of the cysteine moiety. No such adduct was observed in the digestion mixture obtained from vehicle-treated mice. Similar procedure for the synthesis of GSH conjugate **10** was employed to synthesize cysteine adduct **12**. The synthetic cysteine adduct revealed similar retention time and MS/MS spectrum with those of the cysteine adduct observed in animals given compound **1** (Figures 10C/10E).

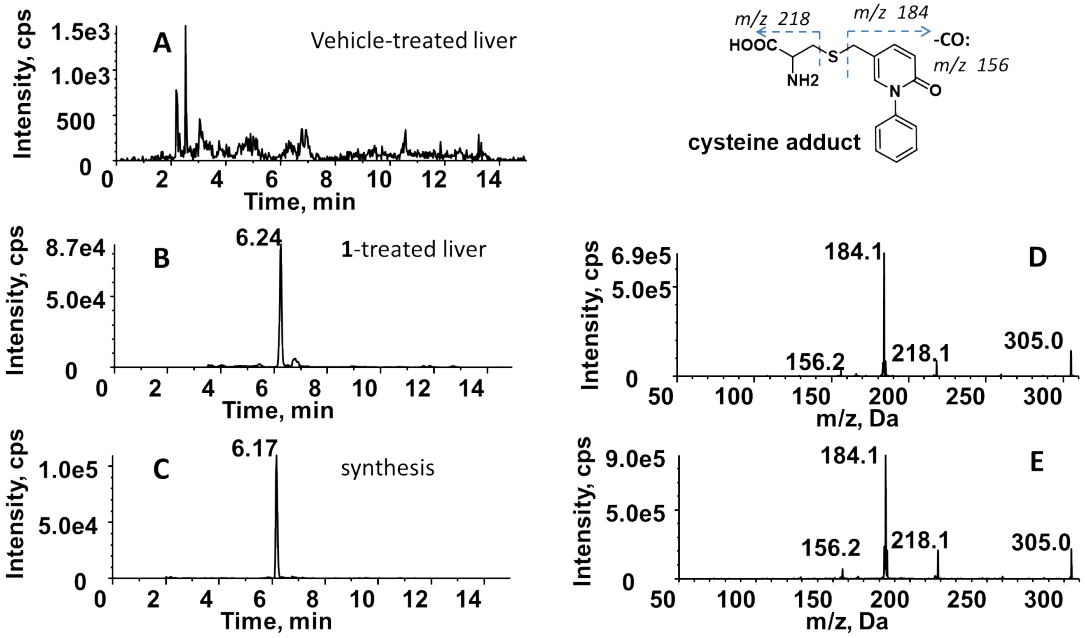

Figure 11. Characterization of cysteine adduct **12**. Extracted ion (*m*/*z* 305/184) chromatograms obtained from LC-MS/MS analysis of proteolytic liver protein samples harvested from vehicle-treated (A) and **1**-treated (B) mice. D: MS/MS spectrum of cysteine adduct **12** obtained from proteolytic liver samples harvested from **1**-treated mice. Extracted ion (*m*/*z* 305/184) chromatogram (C) and MS/MS spectrum (E) of synthetic cysteine adduct **12**.

We examined the time course and dose dependence of the hepatic protein adduction in mice treated with **1**. As depicted in Figure 12A, the hepatic protein adduction reached a peak at 1 h after administration and then diminished in an hour. As expected, the protein adduction increased with the increase of doses administered in mice (Figure 12B).

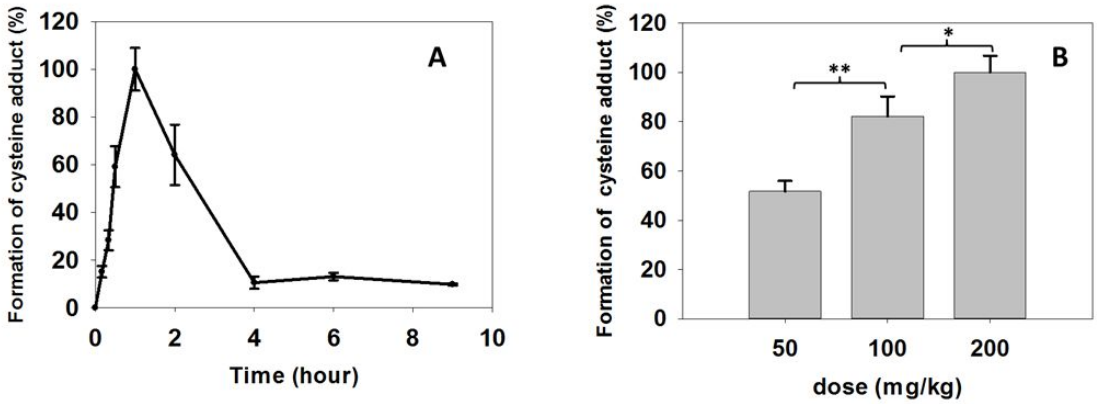

Figure 12. Time course and dose-dependent formation of pirfenidone-derived hepatic protein adduction. A: Levels of cysteine adduct **12** detected in proteolytic liver samples harvested from mice treated with **1** at various time points after administration; B: Levels of cysteine adduct **12** detected in proteolytic liver samples harvested from mice treated with **1** at various doses. Data represent the mean ± SD (n=3). $^{**}p < 0.01$ (mean ± SD).

Furthermore, inhibitors KTC and DCNP were employed to define the roles CYP3A and SULTs in pirfenidone-induced protein modification. As shown in Figure 13, 52% decrease in protein adduction derived from **1** was observed in KTC-pretreated mice. Pretreatment of DCNP also attenuated the protein adduction (by 17%) resulting from the metabolic activation of **1**. This further provides the evidence for the proposed pathways of pirfenidone bioactivation (Scheme 1).

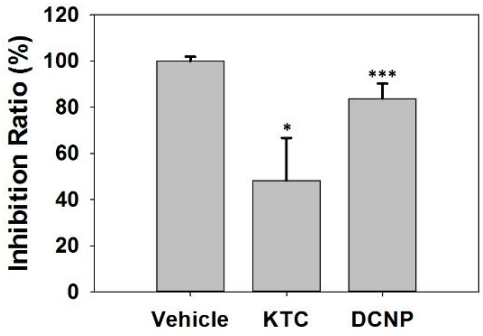

Figure 13. Inhibitory effects of KTC and DCNP on **1**-derived hepatic protein adduction. Levels of cysteine adduct **12** detected in proteolytic liver samples harvested from **1**-treated mice which had respectively been pretreated with vehicle, KTC, or DCNP. Data represent the mean ± SD (n=3). $^{***}p < 0.005$ (mean ± SD)

DISCUSSION AND CONCLUSION

Apparently, pirfenidone does not show severe prototype toxicity in clinic medication but has reportedly revealed adverse effects similar to idiosyncratic reactions (IDRs). Though the mechanisms of IDRs remain uncertain, it has been accepted that metabolic activation is involved in IDRs. Thus, we initiated the study to determine whether metabolic activation of pirfenidone takes place *in vitro* and *in vivo*.

The present study started with microsomal incubations to determine the role of P450s in the metabolic activation of pirfenidone. Pirfenidone **1** was incubated with RLMs fortified with GSH or NAC. Both GSH and NAC are common nucleophilic reagents, with a soft sulfhydryl group, used for trapping electrophilic metabolites generated. And NAC is a supplementary trapping agent to eliminate the interference of glutathione *S*-transferases. Hydroxylated pirfenidone **2** was found to be the primary oxidative metabolite in microsomal incubations. Additionally, GSH conjugate **10** and NAC conjugate **11** were detected in the corresponding incubation systems (Figures 1/2). No such conjugates were observed in NADPH-free microsomal incubations. This indicates that P450s participated in both oxidative metabolism and metabolic activation of pirfenidone.

Chemical synthesis was executed to verify the structure of oxidative metabolite **2** and GSH/NAC conjugates **10**/**11**. To take the advantage of the good leaving group of bromide, P-Br (refer to Experimental Section **2.1.**, Scheme 4) was synthesized as an electrophilic synthon to generate a reactive carbocation. Compound **2** was generated by hydration of P-Br. GSH or NAC was submitted to react with the reactive

carbocation to form conjugates **10/11**. This work assisted us to characterize these metabolites *in vitro* and *in vivo*.

Identification of reactive metabolites is a very important step for mechanistic understanding of the chemistry of metabolic activation. The observed compound **2** allowed us to anticipate that **2** could be dehydrated to quinone methide **3** which sequentially reacts with GSH to generate GSH conjugate **10**. To determine the anticipated dehydration, we incubated **2** with GSH or NAC in buffer systems at pH 5, 7, or 9. We failed to detect any pirfenidone-derived GSH/NAC conjugates in the systems, suggesting that spontaneous dehydration of **2** did not take place even under weak acidic and basic conditions. Furthermore, we incubated **2** with RLMs fortified with GSH or NAC to determine whether cytochrome P450 enzymes would catalyze the formation of quinone methide **3** from **2**. Again, no corresponding GSH/NAC conjugates were detected in the microsomal systems. Clearly, the generation of quinone methide **3** resulted neither from spontaneous dehydration of **2** nor from P450 enzyme-mediated reactions starting from **2** (Scheme 1).

Despite this, metabolic activation of parent compound **1** mediated by P450 enzymes, along with the formation of **2**, is evident. As for the formation of **2**, we proposed that the oxidative reaction is initiated by hydrogen abstraction at the benzylic carbon to form radical **5** (Scheme 2), followed by oxygen rebound. The generation of quinone methide **3** may be achieved by electron transfer of the nitrogen of radical **5** (single electron transfer, SET) to FeO^{3+} of P450 enzymes.[30] Alternatively, SET goes first to produce intermediate **7**, followed by hydrogen abstraction to form quinone

methide **3** (Scheme 2). The reaction of quinone methide **3** with trapping agents GSH/NAC by Michael addition results in the production of conjugates **10/11**.

Scheme 2. Proposed mechanisms of pirfenidone oxidation mediated by P450s.

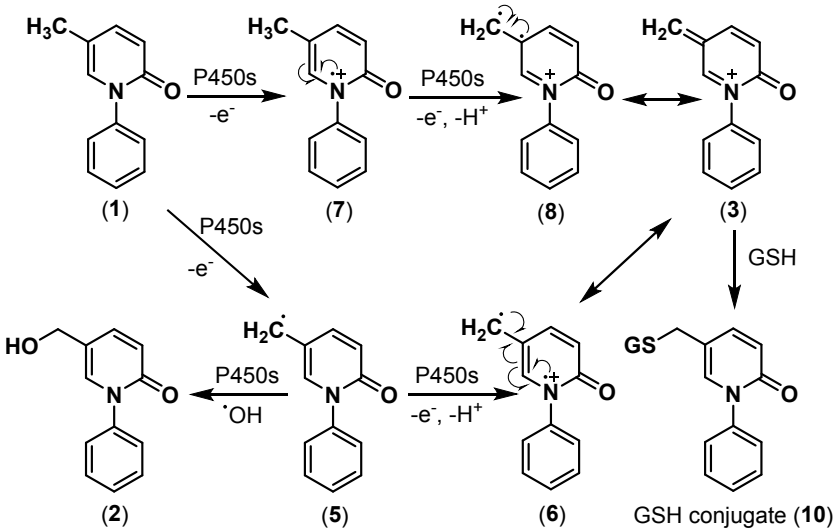

To further define the role of **2** in the metabolic activation, we treated rat primary hepatocytes with **2**. Interestingly, GSH conjugate **10** was detected in the cell culture system but not in NADPH fortified RLMs, suggesting that **2** was bioactivated by non-P450 enzyme systems. As a benzylic alcohol derivative, compound **2** has the possibility to be metabolized by SULTs to sulfate **9** (Scheme 3), a benzyl alcohol-sulfate derivative. Benzyl-sulfates are known to be electrophilic species, due to the departure of sulfonyl group, an excellent leaving group. We speculated that sulfate **9** reacts with GSH to form GSH conjugate **10** (Scheme 3) by S_N1 or/and S_N2 reactions. To probe the hypothesis, we co-treated cells with SULT inhibitor DCNP. The presence of DCNP was found to attenuate the formation of GSH conjugate **10**, indicating the involvement of sulfation in the metabolic activation of **2** (Figure 6A).

Rat liver cytosol incubations supplemented with **2** were carried out, and the formation of GSH/NAC conjugates was found to be PAPS-dependent (Figures 7D/7E and S1D/S1E). This supports the speculated role that the sulfation pathway involves in the metabolic activation of pirfenidone.

Scheme 3. Proposed pathways of metabolic activation of pirfenidone via sulfation.

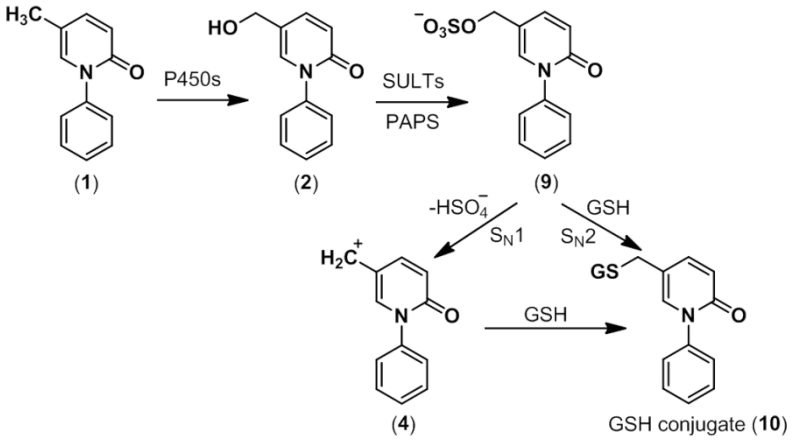

RLM-RLC 2-step incubations were carried out to define the pathway of pirfenidone bioactivation. Pirfenidone was pre-incubated with RLMs in the presence or absence of NADPH, followed by incubation with RLCs spiked with PAPS or vehicle. NADPH was found to be required for the formation of conjugate **10**, and the presence of PAPS elevated the conjugation reaction (Figures 7A/7B/7C). This indicates that P450s initiated the metabolic pathway, and SULTs participated in the rest of pathway (Scheme 3). The observed inhibitory effects of KTC and DCNP in the **1**-treated hepatocyte incubations support the proposed metabolic pathway, suggesting that both oxidation mediated by P450s and sulfation catalyzed by SULTs participated in the metabolic activation of pirfenidone (Figure 6B).

In a recombinant P450 assay, we found that CYP3A4 made the largest contribution to the metabolic activation of **1**, followed by CYP2A6 and CYP1A2 (Figure 4B). Interestingly, CYP1A2 was found to be mainly responsible for the formation of **2** required for the sequential sulfation (Figure S3). Clearly, the expression of CYP1A2 is particularly important to sulfation-mediated metabolic activation of pirfenidone.

Biliary GSH conjugates are generally considered as biomarkers of exposure to electrophilic species. Abundant biliary GSH conjugate **10** found in **1**-treated rats (100 mg/kg, equivalent to its clinical single dosage) provides solid evidence for the formation of electrophilic intermediate *in vivo* (Figure 8). NAC conjugate **11** detected in bile and urine most likely results from further metabolism of GSH conjugate **10**, catalyzed by γ-glutamyltranspeptidase, dipeptidases, and *N*-acetyltransferase.

Protein covalent binding is an important biochemical mechanism for cytotoxicity. Electrophilic species may react with cellular protein, especially when cellular GSH is depleted. The resulting protein modification may cause permanent cellular damages. As for the observed GSH conjugation *in vitro* and *in vivo*, we believed similar chemistry would take place between the reactive intermediates and cysteine residues of protein. The detection of cysteine adduct **12** (Figure 11) in proteolytic protein samples allowed us to verify the protein adduction resulting from the metabolic activation of pirfenidone *in vivo*.

We successfully identified GSH conjugate **10** and NAC conjugate **11**, along with protein covalent binding, resulting from the metabolic activation of pirfenidone. However, we failed to observe liver injury in mice (Figure S4) treated with pirfenidone

at dose of 150 mg/kg (approximately equivalent to its clinical single dosage) and even at 200 mg/kg (Figure S5). In addition, no cytotoxicity was found in cultured primary hepatocytes after exposure to pirfenidone at concentration of 800 μM (Figure S6). It does not necessarily mean that pirfenidone is not hepatotoxic, since no animal models are available for idiosyncratic toxicity investigation. The failure to observe hepatic injury of pirfenidone in regular animals is understandable. The detected quinone methide and sulfate metabolites of pirfenidone are electrophilic, and the two are reactive to nucleophilic sites of cellular molecules. Protein covalent binding resulting from the bioactivation of pirfenidone is evident. Further studies are needed to define the correlation of the protein modification with pirfenidone idiosyncratic toxicities.

In conclusion, our study provided strong evidence for the formation of a quinone methide reactive intermediate from pirfenidone *in vitro* and *in vivo*. The electrophilic species may be generated by two metabolic pathways, including 1) direct oxidation of pirfenidone mediated by P450 enzymes; and 2) hydroxylation of pirfenidone catalyzed by P450 enzymes, followed by SULT-mediated sulfation. The reactive intermediates reacted with sulfhydryl group of cysteine residues to form protein covalent binding. Not only do the findings facilitate the understanding of the mechanisms of the metabolic activation of pirfenidone but also provide medicinal chemists with the information about bioactivation-alerting structure in rational drug design.

EXPERIMENTAL SECTION

1. Chemicals and Materials. Pirfenidone (**1**, >98%) was supplied by Dalian Meilun Biotech Co., Ltd. (Dalian, China). GSH, NAC, cysteine, NADPH, DCNP, dithiothreitol, and KTC were purchased from Aladdin Reagent Co., Ltd. (Shanghai, China). Propranolol, PAPS, and collagenase IV were obtained from Sigma-Aldrich (St. Louis, MO). Pronase E, chymotrypsin, and rat tail collagen I were acquired from SalarBio (Beijing, China). Distilled water was provided by Wahaha Co., Ltd. (Hangzhou, China). All organic solvents were supplied by Fisher Scientific (Springfield, NJ). All the reagents and solvents used were at least of analytical grade.

2.1. 5-Hydroxymethyl-1-phenyl-1H-pyridine-2-one (2). Synthesis of metabolite **2** started with bromination of **1** (Scheme 4), followed by hydration in alkaline aqueous solution. Briefly, compound **1** (185.5 mg, 1.0 mmol) and NBS (178.6 mg, 1.0 mmol) were mixed in 7.0 mL of CCl_4, followed by addition of AIBN (20.0 mg, 0.12 mmol) to trigger the reaction. The reaction mixture was magnetically stirred at 90 °C for 2 h with refluxing, and the reaction was monitored by TLC. The resultant mixture was filtered and the CCl_4 solution was condensed to dryness. Product 5-bromomethyl-1-phenyl-1*H*-pyridine-2-one (P-Br) was reconstituted in 8.0 mL 4 N NaOH and stirred at 40 °C for 4 h. The resulting mixture was submitted to a silica gel chromatography for purification. The product obtained was characterized by Q-TOF MS and NMR. HRMS: *m*/*z* 224.0692 [$C_{12}H_{11}NO_2Na^+$]. According to the prediction formula, the error between the accurate mass and the corresponding theoretical mass was -4.5 ppm. ^{1}H-NMR (DMSO, 600 MHz): δ (ppm) 7.5 (m, 4H), 7.44 (tt, J = 7.4/1.8Hz, 1H), 7.39

(m, 1H), 7.38 (m, 1H), 6.49 (dd, J = 2.4/8.1 Hz, 1H), 5.12 (t, J = 5.3 Hz, 1H,), 4.26 (d, J = 4.7 Hz, 1H). HPLC purity: 98.1%.

Scheme 4. Synthetic route of P-Br.

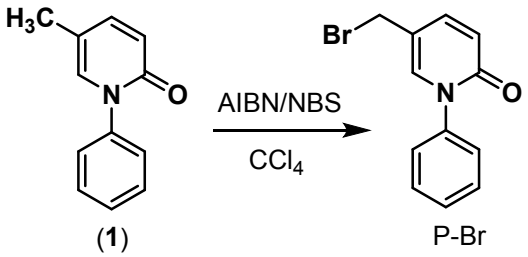

2.2. Synthesis of GSH/NAC/cysteine conjugates (10/11/12). Pirfenidone was brominated as indicated above. The resulting P-Br (26.5 mg, 0.1 mmol) was individually dissolved in 5.0 mL DMSO containing GSH (92.4 mg, 0.3 mmol), NAC (49.0 mg, 0.3 mmol), or cysteine (36.3 mg, 0.3 mmol). The resultant mixtures were stirred at room temperature for 3 h, and the reactions were monitored by LC-MS/MS. The reaction mixture for synthesis of GSH conjugate **10** was submitted to a semi-preparative HPLC system for purification, and the purified product was characterized by HRMS and NMR. HRMS: m/z 491.1595. According to the prediction formula, the error between the accurate mass observed in the HRMS system and the corresponding theoretical mass was 1.2 ppm. ^{1}H-NMR (D_2O, 600 MHz): δ (ppm) 7.8 (dd, J = 2.22/9.29 Hz, 1H), 7.6-7.5 (m, 3H), 7.6 (s, 1H), 7.4 (d, J = 7.33 Hz, 2H), 6.7 (d, J = 9.31 Hz, 1H,), 4.5 (dd, J = 5.34/8.45 Hz, 1H), 3.8 (s, 2H), 3.7 (t, J = 6.43 Hz, 1H), 3.6 (2H, s), 3.0 (dd, J = 5.16/14.2 Hz, 1H), 2.8 (dd, J = 8.64/14.16 Hz, 1H), 2.4 (t, J = 7.67 Hz, 2H), 2.1 (m, 2H). HPLC purity: 95.2%.

3.1. Rat liver microsomal incubations. RLMs were prepared by following a published method.[32] Compound **1** or **2** was dissolved in a phosphate-buffered saline (PBS, 100 mM, pH 7.4) with $MgCl_2$ (3.2 mM). The incubation systems consisted of substrate **1** or **2** at a final concentration of 50 μM, RLMs (final concentration of 1.0 mg protein/mL, assessed by BCA assay), and trapping agents GSH or NAC (1.0 mM). NADPH (2.0 mM) was added to initiate the reactions. NADPH was excluded in control group. The volume of incubation mixtures was 250 μL. After 45 min incubation at 37 °C, the reactions were quenched by addition of 250 μL ice-cold acetonitrile (1:1 v/v). The resultant mixtures were vortex mixed for 2 min and then centrifuged at 19,000 *g* for 10 min. A 3.0 μL aliquot of the resulting supernatants was individually injected into LC-MS/MS for analysis. All incubation reactions were conducted in triplicate. In a separate study, compound **2** was incubated in a buffer system fortified with GSH at pH 5, 7, or 9. The rest of the procedure was the same as that for microsomal incubations described above.

3.2. Recombinant P450 incubations. Incubations of **1** were conducted under similar condition of microsomal incubations described above except that RLMs were replaced by individual human recombinant P450 enzymes (0.1 nM), including CYPs1A2, 2A6, 2B6, 2C9, 2C19, 2D6, 2E1, 3A4, and 3A5. Reactions were terminated by addition of an equal volume of ice-cold acetonitrile containing propranolol (5.0 ng/mL) as the internal standard. The mixture solutions were vortex mixed and centrifuged as described above, and then the supernatants (10 μL) were analyzed by LC-MS/MS.

3.3. Cytosol incubations of 1. RLCs were prepared from rat liver, according to a published method.[33] Liver microsomal incubations (final volume: 100 μL) of **1** were performed as described above, followed by mixing with the secondary incubation mixtures (100 μL) that consisted of GSH/NAC (1.0 mM) and RLCs at a final concentration of 2.0 mg protein/mL. PAPS was added to initiate the sulfation reaction at a final concentration of 250 μM; control reactions were also conducted under the same condition except for the addition of PAPS. The secondary incubations were performed for 45 min at 37 °C. Incubations of **1** with rat liver S9 were also conducted in the presence of NADPH and PAPS. Control groups were performed in the absence of either NADPH or PAPS. Reactions in rat liver S9 were terminated by addition of equal volume of ice-cold acetonitrile after 1 h incubation. Similar protocols were followed for sample preparation as the above. The resulting supernatants (3.0 μL) were analyzed by LC-MS/MS.

3.4. Cytosol incubations of 2. Incubation system contained **2** (50 μM), $MgCl_2$ (3.2 mM), PBS (100 mM, pH 7.4), RLCs (2.0 mg protein/mL), and GSH or NAC (1.0 mM). PAPS (250 μM) was subsequently added to the prepared incubation mixture to lunch the reaction. Control reaction mixture lacked PAPS.

4.1. Animal experiments. All animal experiments were conducted in conformity to regulations authorized by the Ethics Review Committee of Shenyang Pharmaceutical University. Sprague-Dawley rats (220-240 g, male) and Kunming mice (18-22 g, male) were both supplied by the Animal Center of Shenyang Pharmaceutical University.

Animals were housed in a controlled environment (a dark/light cycle for 12 h, a conventional temperature at 21-25 °C, and circulating air change) and were provided with free access to food and water.

4.2. Bile and urine studies. Rats were deprived of food for 12 h and randomly divided to 2 groups. One group of rats were anesthetized by intraperitoneal injection of chloral hydrate (10%) at 5.0 mL/kg. Then animals were treated intraperitoneally with **1** dissolved in saline at 100 mg/kg (the dosage was selected, based on the dose of clinical administration). Bile (0-2 h) was harvested after administration, and blank bile was collected before administration. Separately, rats administered with **1** at the same dose were individually placed in metabolism cages, followed by collecting urine (0-6 h). Blank urine samples were collected before treatment. The animals were allowed to access to water and food 2 h post administration. The collected bile and urine samples were mixed with double volumes of acetonitrile. The mixtures were vortex-mixed and centrifuged at 19,000 *g* for 10 min. The resulting supernatants were analyzed by LC-MS/MS.

4.3. Assessment of hepatic GSH conjugate 10. Mice were fasted for 12 h, randomly divided to 6 groups (3 mice each group), and treated (i.p.) with **1** at 100 mg/kg. Liver samples were harvested at 0 min, 10 min, 30 min, 1 h, 2 h, and 3 h after administration. In a separate study, fasted mice were randomly divided into 10 groups (n=3). Animals were intraperitoneally treated with **1** at 0, 10, 20, 40, 60, 80, 100, 200, 300, or 400 mg/kg, respectively. Liver tissues were harvested after 0.5 h treatment. All of the animals

were anesthetized by diethyl ether before collecting liver. The harvested liver tissues (0.2 g) were homogenized in 0.6 mL PBS and centrifuged at 19,000 *g* for 10 min. The protein contents of the supernatants were measured by BCA assay. Besides, 60 μL of the supernatants were mixed with triple volumes of acetonitrile. The mixtures were vortex mixed and centrifuged at 19,000 *g* for 10 min. The resulting supernatants were analyzed by LC-MS/MS.

4.4. Proteolytic digestion of hepatic protein. Mice were fasted for 12 h and administered (i.v.) with **1** at 100 mg/kg. Liver tissues were respectively harvested at 10 min, 20 min, 30 min, 1 h, 2 h, 4 h, 6 h, and 9 h later (n=3). In a dose-dependent experiment, mice were given **1** intraperitoneally at doses of 0, 50, 100, or 200 mg/kg (n=3), and liver tissues were collected at 1 h after treatment. In a separate study, 12 mice were randomly divided into three groups. One group of mice were pretreated with DCNP (20 mg/kg, i.p.) dissolved in corn oil and then administered with **1** (100 mg/kg, i.p.) dissolved in saline 1 h later; the second group of animals were pretreated with KTC (100 mg/kg, i.p.), followed by administration (i.p.) with **1** at 100 mg/kg 1.5 h later; the third one were treated with **1** 1 h post administration of vehicle (corn oil). At the designed time points, liver tissues (approximately 0.2 g) were harvested, homogenized, and centrifuged at 4,000 *g* for 5 min. The resulting supernatants were heated at 60 °C in a water bath for 30 min. The denatured protein samples were centrifuged at 16,000 *g* for 10 min. The pellets were suspended in 0.1 mL 50 mM NH_4HCO_3 solution (pH=8.0) containing 5.0 mM DTT. After 1 h incubation at 60 °C, the protein samples were digested with a mixture of Pronase E (3.0 mg/mL) and

chymotrypsin (3.0 mg/mL) in the presence of $CaCl_2$ (5.0 mM) by continuous incubating at 37 °C for 12 h. Equal volume of ice-cold acetonitrile containing propranol (5.0 ng/mL) was added to the digestion mixture for protein precipitation. The resulting supernatants were analyzed by LC-MS/MS after centrifugation at 19,000 *g* for 10 min.

5. Primary hepatocyte incubations. Rat primary hepatocytes were isolated by a two-step collagenase perfusion procedure.[34] Briefly, laparotomy surgery was performed in a fasting rat under general anesthesia. An angiocath was inserted into hepatic portal vein for perfusion, and inferior vena cava was cut off to allow efflux of perfusate I and perfusate II. Then the liver was dissected for isolation of hepatocytes, followed by filtration and centrifugation. Cell viability was determined by trypan blue exclusion, which is always higher than 90% eligible for the following experiments. The freshly isolated primary hepatocytes were seeded in 6-well plates pre-coated with rat tail collagen I at a density of 5×10^5 cells/mL. Cells were cultured for 6 h at 37 °C in a humidified incubator (95% O_2 and 5% CO_2). William's complete medium consisted of 20% FBS, 200 units/mL penicillin/streptomycin, 0.5 mg/L insulin, and 0.1 mM dexamethasone. Primary hepatocytes were individually preincubated with DCNP (10 μM), KTC (25 μM), or vehicle (0.1% DMSO, v/v) for 45 min. The resulting cells were washed with PBS, followed by incubation with **1** (100 μM). The resultant culture media and cells were harvested after 1 h incubation. Rat primary hepatocyte incubations of **2** were also conducted in parallel except for the exclusion of KTC pretreatment. The harvested cells, along with culture media, were ultrasonicated for 1 min, followed by addition of double volume of ice-cold acetonitrile containing

propranolol (5.0 ng/mL). The resulting mixtures were vortex mixed, centrifuged, and submitted to LC-MS/MS for analysis.

6. LC-MS/MS methods. LC-MS/MS analyses were performed on an AB SCIEX Instruments 5500 triple quadrupole mass spectrometer coupled to an Agilent 1260 infinity HPLC system with an autosampler. Samples were subjected to chromatographic separation on a ZORBAX SB-C18 reverse-phase column (5.0 μm, 150 mm × 4.6 mm; Agilent Technologies, Santa Clara, CA). Analytes were separated by a linear gradient elution method with mobile phase A (0.1% formic acid) and mobile phase B (acetonitrile containing 0.1% formic acid) at a flow rate of 0.8 mL/min. The gradient program was performed as follows: 0-2 min, 90% A; 2-8min, 90%-10% A; 8-10min, 10% A; 10-12 min, 10% A; 12-15min, 90% A. ESI source was operated in positive ionization mode. Optimal MS parameters were set as follows: source temperature, 650 °C; curtain gas, 35 psi; gas 1, 50 psi; gas 2, 50 psi; ion spray voltage, 5,500 V; entrance potential, 10 V; cell exit potential, 13 V. Multiple-reaction monitoring (MRM) scanning was applied to achieve an appropriate response for the analysis as precursor/product ion pairs (declustering potential, collision energy) at *m*/*z* 186/77 (110, 35), 202/77 (110, 35), 491/184 (100, 30), 347/184 (100, 30), 305/184 (100, 30) and 260/116 (77, 25) for the analysis of **1**, **2**, GSH conjugate **10**, NAC conjugate **11**, cysteine adduct **12**, and propranolol, respectively.

Additionally, enhanced product ion (EPI) scannings in positive mode with a range from *m*/*z* 50 to 500 Da were applied to analyze the fragmentation pattern of the analytes mentioned above by an AB SCIEX Instruments 4000 Q-Trap system coupled to a

Waters ACQUITY™ Ultra Performance LC. The collision energy was set at 35 eV with a spread of 15 eV. EPI was triggered by the information-dependent acquisition (IDA) method for selection of ions acquired more than 1,000 cps with the exclusion of former target ions after three occurrences for 10 s. All data obtained were processed by AB SCIEX Analyst 1.6.2 software (Applied Biosystems, Foster City, CA).

A hybrid Q-TOF mass spectrometer was employed to characterize synthetic **2** and GSH conjugate **10**. Data were processed by Bruker Daltonics Data Analysis 3.4 software.

ASSOCIATED CONTENT

Supporting Information

NAC conjugate **11** generated via sulfation **(**Figure S1**)**; biliary NAC conjugate **11** (Figure S2); P450 enzymes responsible for formation of **2 (**Figure S3**)**; toxicity data (Figures S4/S5/S6).

Molecular string formulas (CSV).

Corresponding Authors

Jiang Zheng, PhD
Wuya College of Innovation, Shenyang Pharmaceutical University, No. 103, Wenhua Road, Shenyang, Liaoning, 110016, P. R. China
State Key Laboratory of Functions and Applications of Medicinal Plants, Key Laboratory of Pharmaceutics of Guizhou Province, Guizhou Medical University, 9 Beijing Road, Guiyang, Guizhou, 550004, P.R. China
Email: zhengneu@yahoo.com
Tel: +86-24-23986361; Fax: +86-24-23986510

Ying Peng, PhD
Wuya College of Innovation, Shenyang Pharmaceutical University, No. 103, Wenhua Road, Shenyang, Liaoning, 110016, P. R. China
Email: yingpeng1999@163.com
Tel: +86-24-23986361; Fax: +86-24-23986510

Weiwei Li, PhD
Guizhou Provincial Key Laboratory of Pharmaceutics, Guizhou Medical University, 9 Beijing Road, Guiyang, Guizhou, 550004, P. R. China
Email: weiweili0615@163.com
Tel: +86-24-23986361; Fax: +86-24-23986510

Funding

This work was supported in part by the National Natural Science Foundation of China [Grants 81773813, 81830104, and U1812403].

Notes

The authors declare no competing financial interests.

ABBREVIATIONS

GSH, glutathione; NAC, *N*-acetyl cysteine; NADPH, *β*-nicotinamide adenine dinucleotide 2'-phosphate reduced tetrasodium salt; SULTs, sulfotransferases; PAPS, 3'-phosphoadenosine-5'-phosphosulfate; KTC, ketoconazole; DCNP, 2, 6-dichloro-4-nitrophenol; P-Br, 5-bromomethyl-1-phenyl-1*H*-pyridine-2-one; LC-MS/MS, liquid chromatography−tandem mass spectrometry; CE, collision energy; DP, declustering potential; EPI, enhanced product ion; IDA, information-dependent acquisition; Q-TOF, quadrupole/time-of-flight.

REFERENCES

(1) Liu, Y. M.; Nepali, K.; Liou, J. P. Idiopathic pulmonary fibrosis: current status, recent progress, and emerging targets. *J. Med. Chem.* **2017**, *60*, 527-553.

(2) Chambers, R. C.; Mercer, P. F. Mechanisms of alveolar epithelial injury, repair, and fibrosis. *Ann. Am. Thorac. Soc.* **2015**, *12*, S16−S20.

(3) Wolters, P. J.; Collard, H. R.; Jones, K. D. Pathogenesis of idiopathic pulmonary fibrosis. *Annu. Rev. Pathol.: Mech. Dis.* **2014**, *9*, 157−179.

(4) Kim, E. S.; Keating, G. M. Pirfenidone: a review of its use in idiopathic pulmonary fibrosis. *Drugs.* **2015**, *75*, 219−230.

(5) Hisatomi, K.; Mukae, H.; Sakamoto, N.; Ishimatsu, Y.; Kakugawa, T.; Hara, S.; Fujita, H.; Nakamichi, S.; Oku, H.; Urata, Y.; Kubota, H.; Nagata, K.; Kohno, S. Pirfenidone inhibits TGF-β1-induced overexpression of collagen type I and heat shock protein 47 in A549 cells. *BMC Pulm. Med.* **2012**, *12*, 24.

(6) Nakazato, H.; Oku, H.; Yamane, S.; Tsuruta, Y.; Suzuki, R. A novel anti-fibrotic agent pirfenidone suppresses tumor necrosis factor-α at the translational level. *Eur. J. Pharmacol*. **2002**, *446*, 177−185.

(7) Misra, H. P.; Rabideau, C. Pirfenidone inhibits NADPH dependent microsomal lipid peroxidation and scavenges hydroxyl radicals. *Mol. Cell. Biochem.* **2000**, *204*, 119−126.

(8) Giri, S. N.; Leonard, S.; Shi, X.; Margolin, S. B.; Vallyathan, V. Effects of pirfenidone on the generation of reactive oxygen species in vitro. *J Environ Pathol Toxicol Oncol.* **1999**, *18*, 169-177.

(9) U.S. Food and Drug Administration. Esbriet (pirfenidone) capsules: US prescribing information. **2014**. https://www.accessdata.fda.gov (accessed September 7, 2019).

(10) National Library of Medicine, the National Insititute of Diabetes and Digestive and Kidney Diseases. Pirfenidone. **2015**. https://livertox.nih.gov/Pirfenidone.htm. (accessed September 7, 2019).

(11) King T. A phase 3 trial of pirfenidone in patients with idiopathic pulmonary fibrosis. *N. Engl. J. Med.* **2014**, *370*, 2083–2092.

(12) Verma, N.; Kumar, P.; Mitra, S.; Taneja, S.; Dhooria, S.; Das, A.; Duseja, A.; Dhiman, R. K.; Chawla, Yogesh. Drug idiosyncrasy due to pirfenidone presenting as acute liver failure: case report and mini-review of the literature. *Hepatol Commun,* **2018**, *2*, 142-147.

(13) Benesic, A.; Jalal, K.; Gerbes, AL. Acute liver failure during pirfenidone treatment triggered by co-medication with esomeprazole. *Hep. (Baltimore, Md.)* **2019**, 1527-3350

(14) Bruss, M. L.; Stanley, S. D.; Margolin, S. B.; Giri, S. N. Pharmacokinetics and metabolism of intravenous pirfenidone in sheep. *Biopharm. Drug. Dispos.* **2008**, *29*, 119-126.

(15) Weinshilboum, R. M. Phenol sulfotransferase in humans: properties, regulation, and function. *Fed Proc.* **1986**, *45*, 2223-2228.

(16) Coughtrie, M. W. H.; Sharp, S.; Maxwell, K.; Innes, N. P. Biology and function of the reversible sulfation pathway catalysed by human sulfotransferases and sulfatases. *Chem Biol Interac.* **1998**, *109*, 3-27.

(17) Falany, C. N. Molecular enzymology of human liver cytosolic sulfotransferases. *Trends Pharmacol Sci.* **1991**, *12*, 255-259.

(18) Coughtrie, M. W. Sulphation catalysed by the human cytosolic sulphotransferases -- chemical defense or molecular terrorism? *Hum Exp Toxicol*, **1996**, *15*, 547-555.

(19) Shimada, T. Xenobiotic-metabolizing enzymes involved in activation and detoxification of carcinogenic polycyclic aromatic hydrocarbons. *Drug Metab Pharmaco kinet*, **2006**, *21*, 257-276.

(20) Li, R.; Li, W.; You, Y.; Guo, X.; Peng, Y.; Zheng, J. Metabolic activation and cytotoxicity of aloe-emodin mediated by sulfotransferases. *Chem Res Toxicol*. **2019**, *32*, 1281−1288.

(21) Ishii, Y., Okamura, T., Inoue, T., Fukuhara, K., Umemura, T., Nishikawa, A. Chemical structure determination of DNA bases modified by active metabolites of lucidin-3-O-primeveroside. *Chem Res Toxicol.* **2010**, *23*, 134-141.

(22) Uetrecht, J. Idiosyncratic drug reactions: past, present, and future. *Chem. Res. Toxicol.* **2008**, *21*, 84–92.

(23) Greene, N.; Fisk L.; Naven, R. T., Note, R. R.; Patel, M. L.; Pelletier D. J. Developing structure-activity relationships for the prediction of hepatotoxicity. *Chem. Res. Toxicol.* **2010**, *23*, 1215–1222.

(24) Uetrecht, J. Idiosyncratic drug reactions: Current understanding. *Annu. ReV. Pharmacol. Toxicol.* **2007,** *47*, 513–539.

(25) Stepan, A. F.; Walker, D. P.; Bauman, J.; Price, D. A.; Baillie, T. A.; Kalgutkar, A. S.; Aleo, M. D.; Structural alert/reactive metabolite concept as applied in medicinal

chemistry to mitigate the risk of idiosyncratic drug toxicity: a perspective based on the critical examination of trends in the top 200 drugs marketed in the united states. *Chem. Res. Toxicol.* **2011,** *24*, 1345–1410.

(26) Nakayama, S.; Atsumi, R.; Takakusa, H.; Kobayashi, Y.; Kurihara, A.; Nagai, Y.; Nakai, D.; Okazaki, O. A zone classification system for risk assessment of idiosyncratic drug toxicity using daily dose and covalent binding. *Drug. Metab. Dispos.* **2009,** *37*, 1970–1977

(27) Phillips, E. J.; Mallal, S. A. Pharmaco genetics of drug hypersensitivity. *Pharmacogenomics.* **2010,** *11*, 973–987.

(28) Uetrecht, J. P. New concepts in immunology relevant to idiosyncratic drug reactions: The "danger hypothesis" and innate immune system. *Chem. Res. Toxicol.* **1999,** *12*, 387–395.

(29) Nelson, S. D. Metabolic activation and drug toxicity. *J. Med. Chem.* **1982,** *25*, 753–765.

(30) Miwa, G. T.; Walsh, J. S.; Kedderis, G. L.; Hollenberg, P. F. The use of intramolecular isotope effects to distinguish between deprotonation and hydrogen atom abstraction mechanisms in cytochrome P-450- and peroxidase-catalyzed N-demethylation reactions. *J. Biol. Chem.* **1983,** *258*, 14445-14449.

(31) Rodrigues, A. D. Integrated cytochrome P450 reaction phenotyping: attempting to bridge the gap between cDNA-expressed cytochromes P450 and native human liver microsomes. *Biochem. Pharmacol.* **1999,** *57*, 465–480.

(32) Lin, D. J.; Li, C. Y.; Peng, Y.; Gao, H. Y.; Zheng, J. Cytochrome P450-mediated metabolic activation of diosbulbin B. *Drug Metab. Dispos.* **2014**, *42*, 1727−1736.

(33) Ma, J. Y.; Zhou, X.; Fu, J. Metabolite profiling analysis of FR429, an ellagitannin purified from polygonum capitatum, in rat and human liver microsomes, cytosol and rat primary hepatocytes in vitro. *Chem Biol Interact.* **2014**, *220*, 33-40.

(34) Shen, L.; Hillebrand, A.; Wang, D.Q.H.; Liu, M. Isolation and primary culture of rat hepatic cells. *J. Vis. Exp.* **2012**, *64*, e3917.

Table of Contents Graphic